

High-Speed Tunnel Injection InGaAs/GaAs Quantum Dot Lasers

P. Bhattacharya* and S. Ghosh
 Department of Electrical Engineering and Computer Science
 University of Michigan, Ann Arbor, MI 48109-2122

ABSTRACT

The design, growth, and steady-state and small-signal modulation characteristics of high-speed tunnel injection $\text{In}_{0.4}\text{Ga}_{0.6}\text{As}/\text{GaAs}$ quantum dot lasers are described and discussed. The measured small-signal modulation bandwidth for $I/I_{\text{th}} \sim 3.2$ is $f_{-3\text{dB}} = 22\text{GHz}$ and the gain compression factor for this frequency response is $\epsilon = 7.2 \times 10^{-16} \text{ cm}^3$. The differential gain obtained from the modulation data is $dg/dn \cong 8.85 \times 10^{-14} \text{ cm}^2$ at room temperature. The value of the K-factor is 0.171ns and the maximum intrinsic modulation bandwidth is 55GHz. The measured high speed data are comparable to, or better than, equivalent quantum well lasers for the first time.

1. INTRODUCTION

Significant milestones in the development of the quantum dot lasers include demonstration of low threshold at room temperature [1], large differential gain [2],[3], high output power [4], wide spectral tunability [5] and better temperature insensitivity of the threshold current [6],[7] than quantum well lasers. However, it is now clear that the carrier dynamics in quantum dots do not favor high speed operation, such as direct modulation, of lasers [3],[8]-[12]. More specifically, detailed two- and three-pulse pump-probe differential transmission spectroscopy measurements made by us on quantum dot (QD) heterostructures show that at temperatures above 100K, a large number of injected electrons preferentially occupy the higher lying states of the dots and states in the adjoining barrier/wetting layer with higher density [13],[14]. Additionally a phonon bottleneck has also been observed in the same QD heterostructures, when electrons and holes are non-geminately captured (in different dots) [15]. Therefore, there exists a significant hot-carrier problem in QD lasers. We attribute this to be the principal reason for the inability to modulate QD lasers at high speeds. The technique of tunnel injection in semiconductor lasers was proposed and demonstrated almost a decade ago to alleviate problems related to hot carriers in the active region and surrounding layers. By tunneling "cold" electrons directly into the lasing states of GaAs- and InP- based quantum well lasers from an adjacent injector layer, the performance characteristics were enhanced and several deleterious effects were minimized [16].

The tunneling injection (TI) scheme can be applied to quantum dot lasers, whereby electrons can be transported directly to the lasing states in the dots. Theoretical calculations made by Asryan and Luryi [17] indicate that large values of T_0 may be obtained in QD-TI lasers due to a minimization of carrier leakage from the active region and reduced parasitic recombination in the optical confinement layer and hot-carrier effects in the devices. By careful engineering of the QD heterostructure, we have demonstrated large modulation bandwidths in InGaAs/GaAs self-organized QD lasers at room temperature, for the first time [18]. These lasers also demonstrate ultra-low chirp ($< 0.5\text{\AA}$), α -factors ~ 1 [18], and T_0 as high as 363K around room temperature [19]. Advantages of using the tunneling scheme have also been reported for self-organized InP/InAlP QD lasers [20].

*pkb@eecs.umich.edu; phone 1-734-763-6678; fax 1-734-763-9324

2. MBE GROWTH OF TUNNELING INJECTION LASER

The laser heterostructure, designed with knowledge of the quantum dot electronic states, is shown in Fig. 1(a). The device structure consists of 1.5 μm thick $\text{Al}_{0.55}\text{Ga}_{0.45}\text{As}$ outer cladding layers ($n,p = 5 \times 10^{17} \text{ cm}^{-3}$) and GaAs contact layers on either side of the 0.15 μm thick undoped GaAs optical confinement layer (OCL). The active region consists of the $\text{In}_{0.25}\text{Ga}_{0.75}\text{As}$ injector well, a 20 \AA $\text{Al}_{0.55}\text{Ga}_{0.45}\text{As}$ tunnel barrier and three coupled $\text{In}_{0.4}\text{Ga}_{0.6}\text{As}$ QD layers. The 95 \AA $\text{In}_{0.25}\text{Ga}_{0.75}\text{As}$ injector well is grown at 490 $^{\circ}\text{C}$, the QD layers are grown at 525 $^{\circ}\text{C}$ and the rest of the structure is grown at 620 $^{\circ}\text{C}$. The conduction band profile in the active region is shown in Fig. 1(b). A critical aspect of the design is the alignment of the conduction band states of the injector layer with the bound states in the quantum dots, such that efficient phonon-assisted tunneling can take place from the injector layer to the dots. The bandgap of the injector layer is tuned for the optimum tunneling conditions and the tunneling rates are measured, as described in the next section. The wavelength of the luminescence peak for the dots is controlled by adjusting the InGaAs dot charge during epitaxy such that the energy separation, in the conduction band, between the injector well states and the QD ground states is ~ 36 meV at room temperature (see Fig. 2). This energy separation ensures LO phonon-assisted tunneling from the injector well to the dot ground states through the 20 \AA undoped $\text{Al}_{0.55}\text{Ga}_{0.45}\text{As}$ barrier layer. The injected holes rapidly thermalize to the dot ground states and the $\text{Al}_{0.55}\text{Ga}_{0.45}\text{As}$ barrier prevents hole injection and recombination in the injector layer. Single-mode ridge waveguide lasers of cavity lengths varying from 200-1300 μm were fabricated by standard lithography, wet and dry etching, and metallization techniques. The devices were mounted on Cu heat sinks for the measurements. The cleaved facets were left uncoated for the measurements reported here.

3. DEVICE CHARACTERISTICS

3.1 DC Characteristics

The steady-state characteristics of the lasers were measured under pulsed conditions (1 μs pulses and 1% duty cycle) as a function of temperature and for various cavity lengths. Typical light-current characteristics for a 400 μm long device is shown in Fig. 3(a). At room temperature (288K) the lasers are characterized by $I_{\text{th}} = 8\text{mA}$ ($l = 400\mu\text{m}$), $J_{\text{th}} = 520\text{A}/\text{cm}^2$ ($l = 1300\mu\text{m}$), high slope efficiency ($\sim 0.9\text{W}/\text{A}$ for $l = 200\mu\text{m}$) and high differential quantum efficiency ($\eta_{\text{d}} = 0.73$ for $l = 400\mu\text{m}$). From a plot of $1/\eta_{\text{d}}$ versus l shown in Fig. 3(b), values of internal quantum efficiency $\eta_{\text{i}} = 0.85$ and cavity loss coefficient $\gamma = 8.2\text{cm}^{-1}$ are obtained. As shown in Fig. 4, from the measured threshold currents at different temperatures, values of $T_0 = 363\text{K}$ for $5^{\circ}\text{C} < T < 60^{\circ}\text{C}$ and $T_0 = 202\text{K}$ for $60^{\circ}\text{C} < T < 100^{\circ}\text{C}$ are derived. These are the highest values of T_0 measured in these temperature ranges in quantum dot lasers. The high device efficiencies and the high values of T_0 indicate minimization of carrier leakage from the gain region and parasitic recombination in optical confinement layers.

5.2 Small-Signal Modulation Characteristics

The small-signal modulation response of the devices was measured with another set of devices at room temperature under cw biasing conditions with a HP 8562A electrical spectrum analyzer, a HP 8350B sweep oscillator, a low noise amplifier, and a New Focus high-speed detector. The frequency response for varying injection currents for a 400 μm long laser cavity ($I_{\text{th}}(\text{cw}) = 12\text{mA}$) is shown in Fig. 5(a). The continuous lines are best fit curves to the measured data. The spectral outputs at these injection currents confirm that lasing from the ground state is maintained. A bandwidth of $f_{-3\text{dB}} = 22\text{GHz}$ is measured for $I \sim 42\text{mA}$ and this is the highest bandwidth measured in any QD laser at room temperature. Figure 5(b) shows the plot of the resonance frequency f_r of the modulation response as a function of the square root of the output power. The modulation efficiency, which is the slope of this plot, is $\sim 2.6 \text{ GHz}/\text{mA}^{1/2}$. From this value of the modulation efficiency and using a fill factor of $\sim 28\%$, internal quantum efficiency $\eta_{\text{i}} \sim 0.88$ (for the measured device) and a confinement factor $\Gamma \sim 2.5 \times 10^{-3}$, we derive a value of $dg/dn \cong 8.85 \times 10^{-14} \text{ cm}^2$ at room temperature. A value of $K = 0.17\text{ns}$ was calculated using the damping factor obtained from the best fit curves to the measured modulation response. Using the values of K and cavity photon lifetime, we get a gain compression factor, ϵ , of $\sim 7.2 \times 10^{-16} \text{ cm}^3$. A maximum intrinsic modulation bandwidth of 55 GHz is also obtained from this value of K .

The linewidth enhancement factors as function of frequency were obtained by measuring the subthreshold emission spectra of the single-mode tunnel injection ridge waveguide lasers and by calculating the Fabry-Perot mode peak-to-valley ratios and shifts between two differential bias currents. The Fabry-Perot mode shifting due to heating was minimized by using a pulsed bias (1 μ s pulse width and 10KHz repetition rate). Shown in Fig. 6(a) is the wavelength (frequency) dependence of the linewidth enhancement factor. We measure a maximum value of $\alpha \cong 1.2$ at the lasing wavelength. These values of α , which agree with those reported by Newell et. al.[21] for SCH-QD lasers, suggest that the emission linewidth of these quantum dot lasers approaches the Schawlow-Townes limit. The observed trend in the data as a function of wavelength is explained by the fact that in the tunnel injection laser, most of the carriers are injected into the lasing state and the carrier distribution remains quasi-Fermi. Therefore, the carrier induced refractive index change is expected to be a maximum at or near the lasing wavelength. The values of α are a factor of 2-5 lower than those measured in SCH quantum well lasers [22] and this is largely attributed to the higher differential gain and a smaller carrier-induced modulation of the refractive index in the active volume.

The chirp in a semiconductor laser is directly proportional to the linewidth enhancement factor α . We have measured the chirp in the tunnel injection QD lasers during direct small-signal modulation at room temperature by measuring the broadening of a single longitudinal mode using an optical spectrum analyzer. Lasing was confirmed to be at the ground state wavelength. The sinusoidal modulation current was superimposed on a pulsed dc bias current. The envelope of the dynamic shift in the wavelength was recorded and the difference between the half-width of the observed envelope with and without modulation was used to evaluate the chirp. The resolution of the optical spectrum analyzer was 0.08nm. The measurements were first done at a frequency of 5GHz with a pulsed DC bias of 28mA and the peak-to-peak modulation current (I_{p-p}) was varied from 4.2mA to 42mA. The data are shown in Fig. 6(b). Chirp in a In_{0.25}Ga_{0.75}As SCH quantum well lasers of identical cavity dimensions and having a similar threshold current was also measured under identical conditions and the data are also displayed in Fig. 6(b). The values of chirp in quantum well laser are comparable to those reported earlier [23]. In Fig. 6(c) we show the measured chirp in the quantum dot devices as a function of modulation frequency. It is evident from the data of Figs. 6(b) and (c) that chirp in the tunnel injection QD lasers is almost non-existent and at the noise level of the measurements, even at high modulation frequencies. This behavior also confirms the reduction in hot carrier density in the active volume of the lasers. The low chirp also follows from the small linewidth enhancement factor in these devices.

4. CONCLUSION

In conclusion, we demonstrate enhanced performance characteristics in tunnel injection In_{0.4}Ga_{0.6}As/GaAs self-organized quantum dot lasers. Large values of T_0 and high slope and differential quantum efficiencies in these devices are attributed to the cold carrier injection and distribution maintained by the tunneling scheme in these devices. We have measured extremely fast temperature independent tunneling times (~1-2ps). We also demonstrate extremely high modulation bandwidths, exceeding 20GHz, at room temperature. These data, together with our measured values of chirp ~ 0.5Å and linewidth enhancement factor $\alpha = 1.2$ at the lasing wavelength [32], make the tunnel injection quantum dot lasers serious contenders as high performance sources for optical communication.

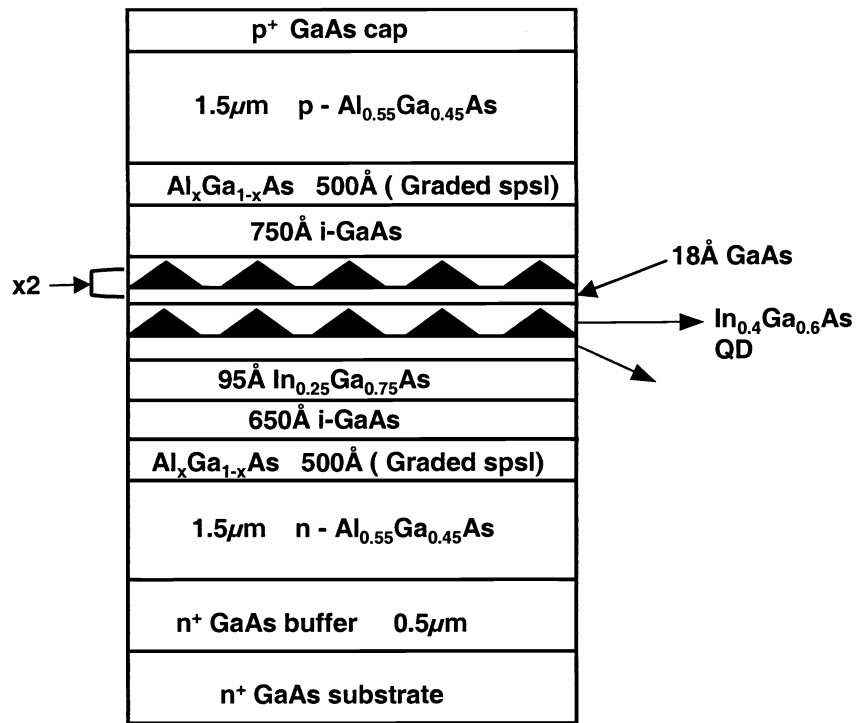
5. ACKNOWLEDGEMENTS

The authors thank Professor D. Bimberg for useful discussions. The work was supported by the Army Research Office under grant DAAD019-01-1-0331.

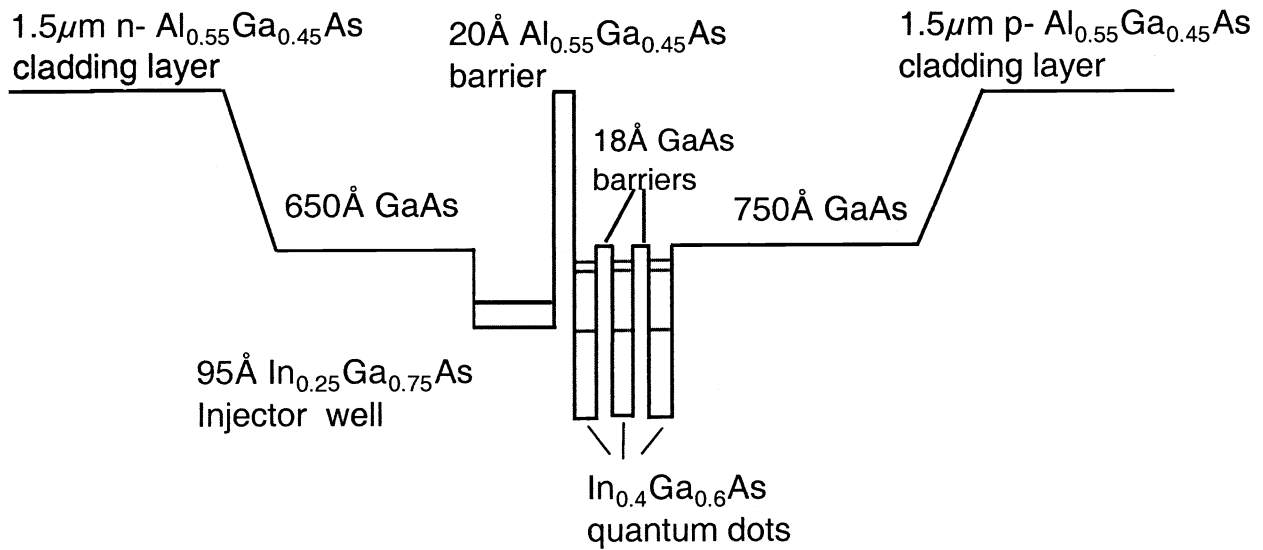
REFERENCES

- [1]. G.T. Liu, A. Stintz, H. Li, K.J. Malloy, and L.F. Lester, "Extremely low room-temperature threshold current density diode lasers using InAs dots in In_{0.15}Ga_{0.85}As quantum well," *Electron. Lett.*, **35**, pp. 1163-1165, 1999.
- [2]. N. Kirstaedter, O. Schmidt, N. Ledentsov, D. Bimberg, V. Ustinov, A. Egorov, A. Zhukov, M. Maximov, P. Kop'ev, and Zh. I. Alferov, "Gain and differential gain of single layer InAs/GaAs quantum dot injection lasers," *Appl. Phys. Lett.*, **69**, pp. 1226-1228, 1996.

- [3]. D. Klotzkin, K. Kamath, K. Vineberg, P. Bhattacharya, R. Murty, and J. Laskar, "Enhanced modulation bandwidth (20 GHz) of $\text{In}_{0.4}\text{Ga}_{0.6}\text{As}/\text{GaAs}$ self-organized quantum-dot lasers at cryogenic temperatures: role of carrier relaxation and differential gain," *IEEE Photon. Technol. Lett.*, **10**, pp. 932-934, 1998.
- [4]. D. Bimberg, M. Grundmann, F. Heinrichsdorff, N. N. Ledentsov, V. M. Ustinov, A. E. Zhukov, A. R. Kovsh, M. V. Maximov, Y. M. Shernyakov, B. V. Volovik, A.F. Tasul'nikov, P.S. Kop'ev, Zh. I. Alferov, "Quantum dot lasers: breakthrough in optoelectronics," *Thin Solid Films*, **367**, pp. 235-249, 2000.
- [5]. P.M. Varangis, H. Li, G.T. Liu, T.C. Newell, A. Stintz, B. Fuchs, K.J. Malloy, and L.F. Lester, "Low-threshold quantum dot lasers with 201 nm tuning range," *Electron. Lett.*, **36**, pp. 1544-1545, 2000.
- [6]. M. V. Maksimov, N. Yu. Gordeev, S. V. Zaitsev, P. S. Kop'ev, I. V. Kochnev, N. N. Ledentsov, A. V. Lunev, S. S. Ruvimov, A. V. Sakharov, A. F. Tsatsul'nikov, Yu. M. Shernyakov, Zh. I. Alferov, and D. Bimberg, "Quantum dot injection heterolaser with ultrahigh thermal stability of the threshold current up to 50 °C," *Semiconductors*, **31**, pp. 124-126, 1997.
- [7]. O. B. Shchekin and D. G. Deppe, "1.3 μm InAs quantum dot laser with $T_o = 161$ K from 0 to 80 °C," *Appl. Phys. Lett.*, **80**, pp. 3277-3299, 2002.
- [8]. K. Kamath, J. Phillips, H. Jiang, J. Singh, and P. Bhattacharya, "Small-signal modulation and differential gain of single-mode self-organized $\text{In}_{0.4}\text{Ga}_{0.6}\text{As}/\text{GaAs}$ quantum dot lasers," *Appl. Phys. Lett.*, **70**, pp. 2952-2953, 1997.
- [9]. D. Klotzkin, K. Kamath, and P. Bhattacharya, "Quantum capture times at room temperature in high-speed $\text{In}_{0.4}\text{Ga}_{0.6}\text{As}-\text{GaAs}$ self-organized quantum dot lasers," *IEEE Photonics Technol. Lett.*, **9**, pp. 1301-1303, 1997.
- [10]. P. Bhattacharya, K. K. Kamath, J. Singh, D. Klotzkin, J. Phillips, H. Jiang, N. Chervela, T. B. Norris, T. Sosnowski, J. Laskar, and M. R. Murty, "In(Ga)As-GaAs self-organized quantum dot lasers: DC and small-signal modulation properties," *IEEE Trans. Electron. Dev.*, **46**, pp. 871-883, 1999.
- [11]. D. Klotzkin and P. Bhattacharya, "Temperature dependence of dynamic and DC characteristics of quantum well and quantum-dot lasers: a comparative study," *J. Lightwave Technol.*, **17**, pp. 1634-1642, 1999.
- [12]. P. Bhattacharya, D. Klotzkin, O. Qasaimah, W. Zhou, S. Krishna, and D. Zhu, "High-speed modulation and switching characteristics in In(Ga)As-GaAs self-organized quantum-dot lasers," *IEEE J. Selected Topics Quantum Electron.*, **6**, pp. 426-438.
- [13]. J. Urayama, T.B. Norris, H. Jiang, J. Singh, and P. Bhattacharya, "Temperature-dependent carrier dynamics in self-assembled InGaAs quantum dots," *Appl. Phys. Lett.*, **80**, pp. 2162-2164, 2002.
- [14]. K. Kim, J. Urayama, T. B. Norris, J. Singh, J. Phillips, and P. Bhattacharya, "Gain dynamics and ultrafast spectral hole burning in In(Ga)As self-organized quantum dots," *Appl. Phys. Lett.*, **81**, pp. 670-672, 2002.
- [15]. J. Urayama, T. Norris, J. Singh, and P. Bhattacharya, "Observation of Phonon Bottleneck in Quantum Dot Electronic Relaxation," *Phys. Rev. Lett.*, **86**, pp. 4930-4933, 2001.
- [16]. P. Bhattacharya, J. Singh, H. Yoon, Xiangkun, Zhang, A. Gutierrez-Aitken, and Y. Lam, "Tunneling injection lasers: a new class of lasers with reduced hot carrier effects," *IEEE J. Quantum Electron.*, **32**, pp. 1620-1629, 1996.
- [17]. L. Asryan and S. Luryi, "Tunnel-injection quantum-dot laser: ultra-high temperature stability," *IEEE J. Quantum Electron.*, **37**, pp. 905-910, 2001.
- [18]. S. Ghosh, S. Pradhan, and P. Bhattacharya, "Dynamic characteristics of high-speed $\text{In}_{0.4}\text{Ga}_{0.6}\text{As}/\text{GaAs}$ self-organized quantum dot lasers at room temperature," *Appl. Phys. Lett.*, **81**, 3055-3057 (2002).
- [19]. S. Pradhan, S. Ghosh, and P. Bhattacharya, "Temperature dependent steady-state characteristics of high-performance tunnel injection quantum dot lasers," *Electron. Lett.* (accepted for publication).
- [20]. G. Walter, N. Holonyak Jr., J. H. Ryou, and R. D. Dupuis, "Coupled InP quantum-dot InGaP quantum well InP-InGaP-In(AlGa)P-InAlP heterostructure diode laser operation," *Appl. Phys. Lett.*, **79**, pp. 3215-3217, 2001.
- [21]. T.C. Newell, D.J. Bossert, A. Stintz, B. Fuchs, K.J. Malloy, and L.F. Lester, "Gain and linewidth enhancement factor in InAs quantum-dot laser diodes," *IEEE Photon. Technol. Lett.*, **11**, pp. 1527-1529 (1999).
- [22]. J. Stohs, D. Bossert, D. Gallant, and S. Brueck, "Gain, refractive index change, and linewidth enhancement factor in broad-area GaAs and InGaAs quantum-well lasers," *IEEE J. Quantum Electron.*, **37**, 1449-1459 (2001).
- [23]. H. Saito, K. Nishi, S. Sugou, "Low chirp operation in 1.6 μm quantum dot laser under 2.5 GHz direct modulation," *Electron. Lett.*, **37**, 1293-1295 (2001).



(a)



(b)

Figure 1 (a) Tunnel injection quantum dot laser heterostructure grown by molecular beam epitaxy; (b) conduction band profile under flat-band conditions.

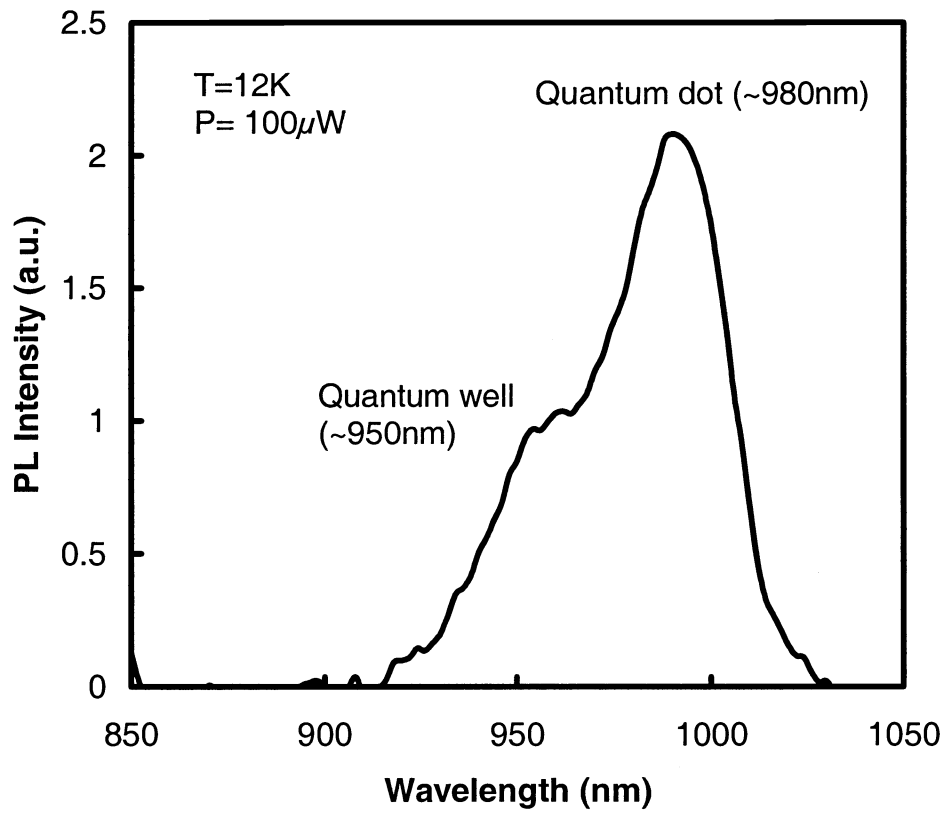


Figure 2 (a) Low temperature photoluminescence spectrum of the tunnel injection laser

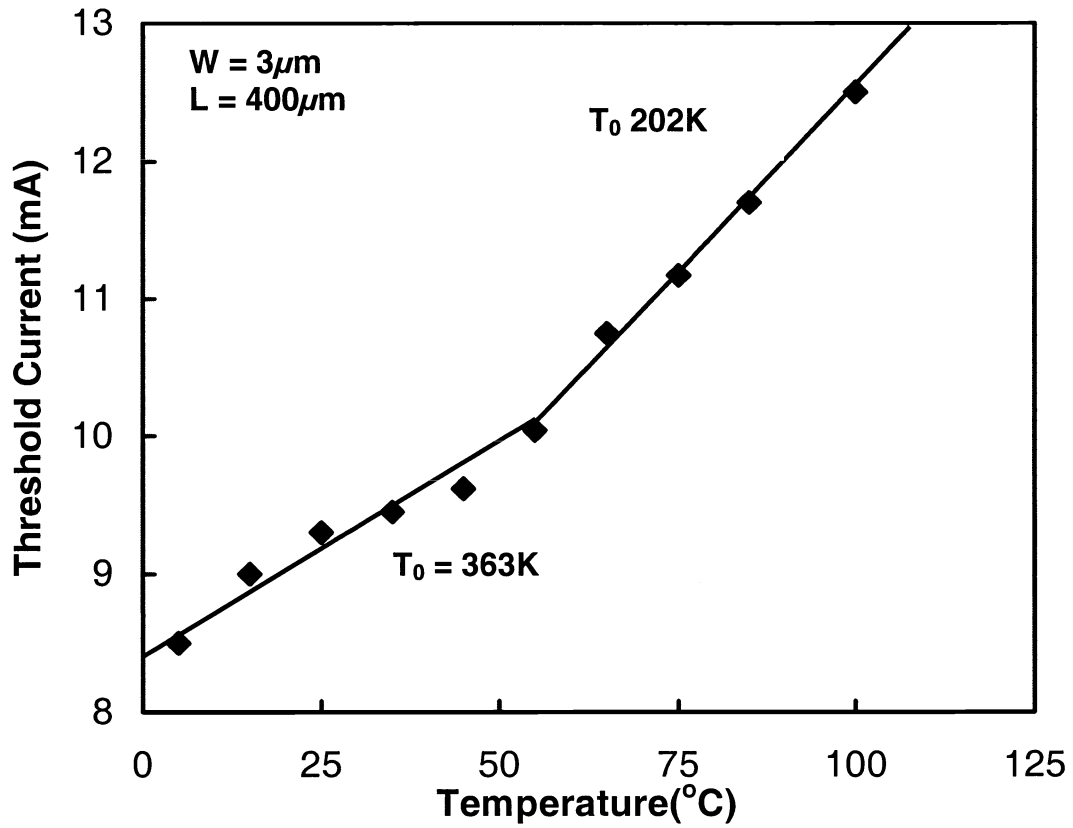
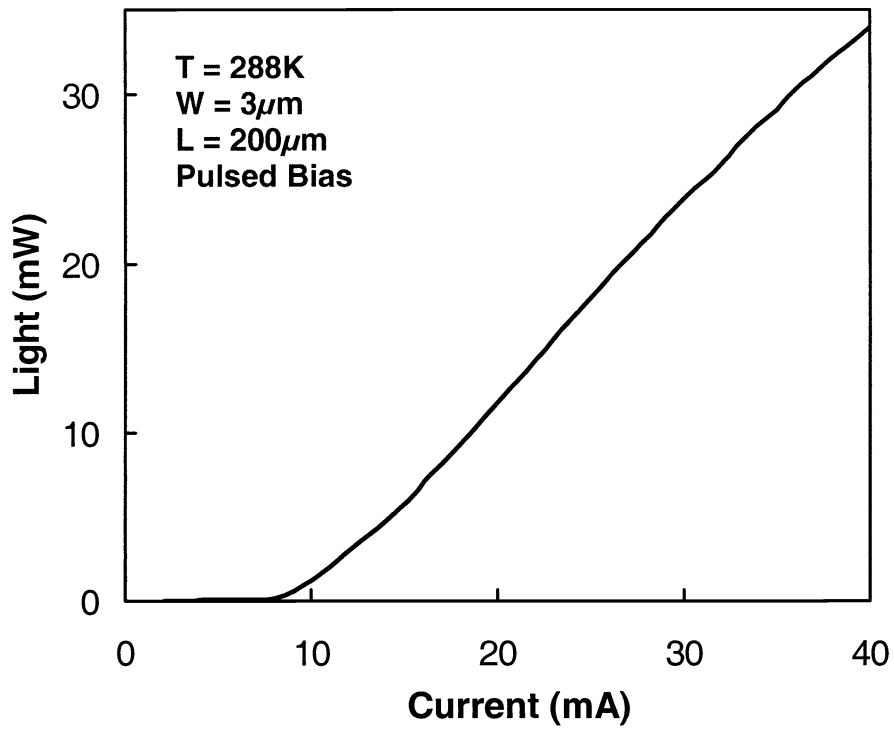
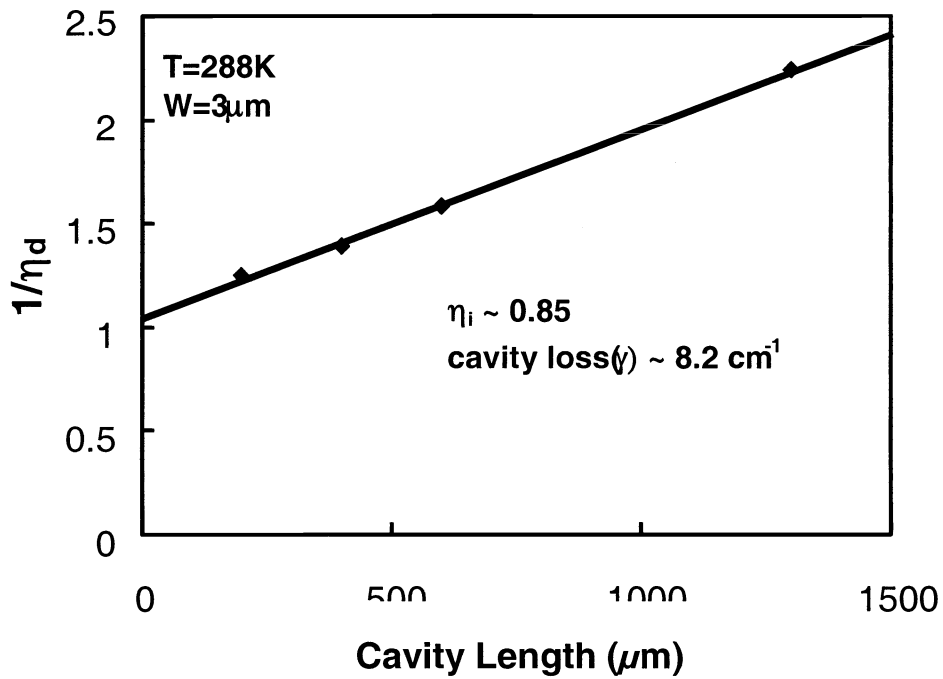


Figure 3 (a) Measured light-current characteristics of a $200\mu m$ long single-mode tunnel injection quantum dot laser at room temperature; (b) plot of inverse differential quantum efficiency vs. cavity length.

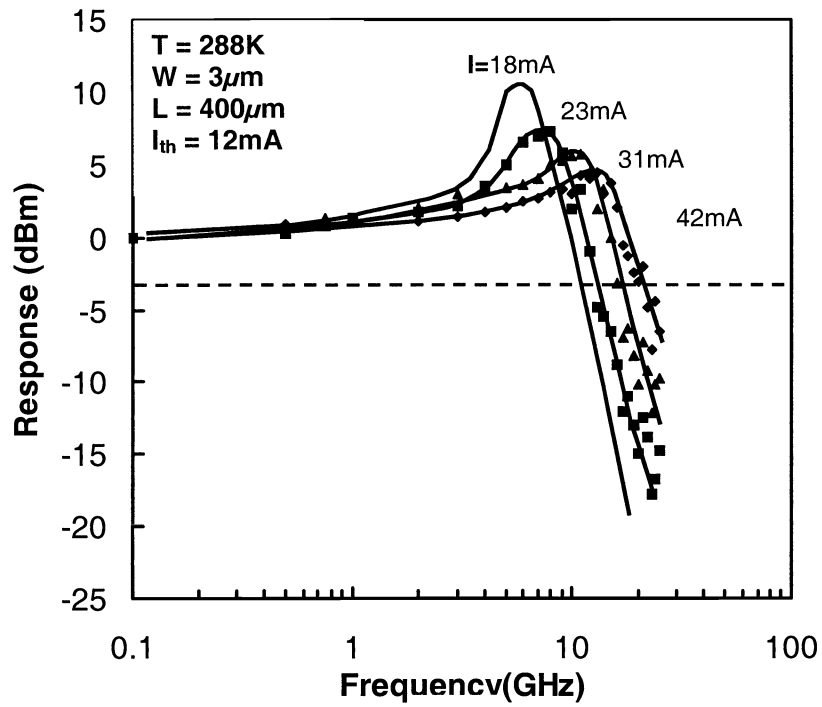


(a)

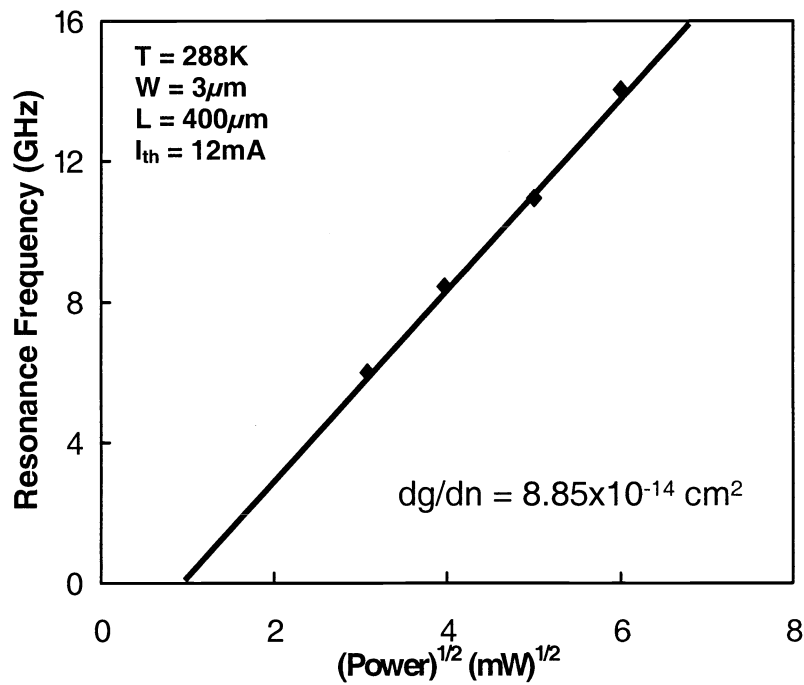


(b)

Figure 4 Variation of I_{th} with temperature. The lines are fit to the data in accordance with $I_{th}(T) = I_{th}(0)e^{T/T_0}$.

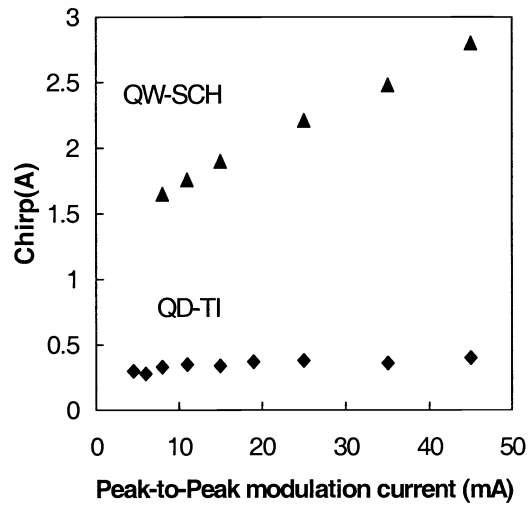
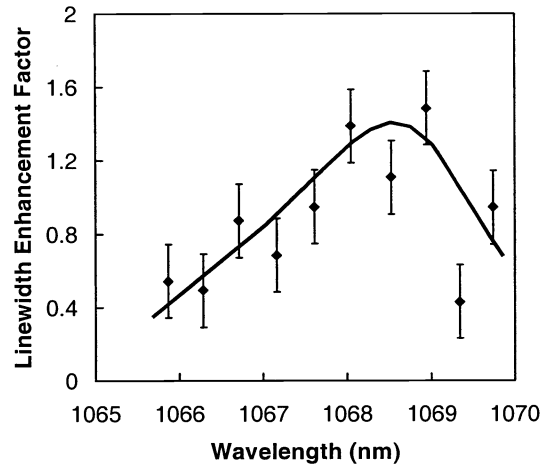


(a)

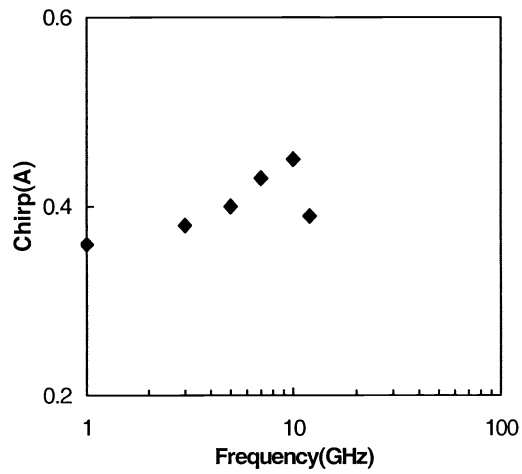


(b)

Figure 5 (a) Small-signal modulation response of 400 μm long tunnel injection laser under varying injection currents at room temperature; (b) the plot of resonance frequency f_r of the modulation response versus square root of injection current $(I - I_{th})$.



(b)



(c)

Figure 6 (a). Measured linewidth enhancement factor versus wavelength; (b) plots of measured chirp in the tunnel injection quantum dot laser and a SCH quantum well laser as a function of modulation current; (c) measured chirp as a function of modulation frequency in a tunnel injection quantum dot laser.